

A new experimental setup to measure hydraulic conductivity of plant segments

3

4

February 24, 2023

1 Abstract

6 Plant hydraulic conductivity and its decline under water stress is the focal point
7 of current plant hydraulic research. Common methods of measuring hydraulic
8 conductivity control a pressure gradient to push water through plant samples,
9 submitting them to conditions far away from those that are experienced in na-
10 ture where flow is suction driven and determined by the leaf water demand. In
11 this paper, we present two methods for measuring hydraulic conductivity under
12 closer to natural conditions, an artificial plant setup, and a horizontal syringe
13 pump setup. Both approaches use suction to pull water through a plant sample
14 while dynamically monitoring flow rate and pressure gradients. The syringe
15 setup presented here allows for controlling and rapidly changing flow and pres-
16 sure conditions, enabling experimental assessment of rapid plant hydraulic re-
17 sponses to water stress. The setup also allows quantification of dynamic changes
18 in water storage of plant samples. Our tests demonstrate that the syringe pump
19 setup can reproduce hydraulic conductivity values measured using the current
20 standard method based on pushing water under above-atmospheric pressure.
21 Surprisingly, using both the traditional and our new syringe pump setup, we
22 found a positive correlation between changes in flow rate and hydraulic con-
23 ductivity. Moreover, when flow or pressure conditions were changed rapidly,
24 we found substantial contributions to flow by dynamic and largely reversible
25 changes in the water storage of plant samples. Although the measurements can
26 be performed under sub-atmospheric pressures, it is not possible to subject the
27 samples to negative pressures due to the presence of gas bubbles near the valves
28 and pressure sensors. Regardless, this setup allows for unprecedented insights
29 into the interplay between pressure, flow rate, hydraulic conductivity, and wa-

30 ter storage in plant segments. This work was performed using an Open Science
31 approach with the original data and analysis to be found at (LINK TO BE
32 ADDED BEFORE PUBLICATION)

33 2 Background and Aims

34 Plant leaves absorb light and CO_2 for photosynthesis, but at the same time
35 they lose water to the atmosphere through transpiration. To replenish water
36 loss, plants entertain an elaborate network of xylem conduits that connect the
37 water uptake tissues in the roots with the evaporating tissues in the leaves.
38 Similarly to porous media, water loss causes tension in the leaves, which drives
39 root-leaf water transport along the pressure gradient between the leaves and
40 the roots, supported by cohesion between water molecules. This is commonly
41 described as the cohesion-tension theory (Dixon and Joly, 1895; Zimmermann
42 et al., 1993; Tyree and Zimmermann, 2002; Shi et al., 2020).

43 Plant water transport through xylem can only be maintained if the pressure
44 drop between roots and leaves is greater than the hydrostatic pressure drop due
45 to the change in gravitational potential between roots and leaves. The drier
46 the soil, the larger the tension in the soil itself, requiring even more tension (or
47 lower water pressure) in the leaves to ensure water transport (Dixon and Joly,
48 1895). These pressures in the xylem are commonly so low that the system is
49 believed to operate in a meta-stable state, where any air seeding in a vessel
50 can cause embolism propagation, resulting in embolisms, which would make a
51 vessel dysfunctional for water transport (Sperry, 1986; Canny, 1998). Here we
52 refer to air seeding as any process that introduces air into the xylem (Tyree and
53 Zimmermann, 2002), such as air entry through pit membranes or wounds.

54 The presence of embolized conduits reduces the efficiency of water trans-
55 port, expressed as a decrease in hydraulic conductivity. The reduced hydraulic
56 conductivity due to embolism has to be compensated for by an increased pres-
57 sure gradient, i.e. lower water pressures in the xylem, in order to maintain
58 an adequate water transport rate. The lower pressure can lead to more em-
59 bolized conduits, resulting in the positive feedback loop of runaway embolism
60 propagation (Tyree and Sperry, 1988; Hölttä et al., 2009).

61 Vulnerability of a plant to embolism spreading and loss of hydraulic conduc-
62 tivity is a primary focus in current plant hydraulic research (McDowell et al.,
63 2019). Many methodological advances have been made to measure the “percent

64 loss of hydraulic conductivity” (PLC) under water stress, but the methods to
65 measure exact hydraulic conductivity values in plants or plant segments have
66 received relatively little scrutiny (see, e.g. Cochard et al., 2013; Venturas et al.,
67 2017).

68 In the most common method for measuring plant hydraulic conductivity,
69 one end of the plant sample is attached to a tube with above-atmospheric liquid
70 pressure (e.g. a water reservoir that is elevated), while the other is exposed to
71 atmospheric pressure, where water flows into a reservoir placed on a balance.
72 The change in weight of the downstream reservoir over time is used to calculate
73 the flow generated by the hydraulic head. In this paper we will refer to this
74 method as the “Sperry method” (Sperry et al., 1988; Canny et al., 2007; Torres-
75 Ruiz et al., 2012). A slight modification to this method was employed by Tyree
76 and Yang (1992), who added a balance under the supplying reservoir, allowing
77 to quantify gains in sample water content during refilling of desiccated samples
78 under pressure. A similar technique to the Sperry method uses a high pressure
79 flow meter (HPFM), where pressure is generated on one side using compressed
80 air to push water through a plant sample connected by flexible tubing. The
81 flow is calculated from the pressure drop across a capillary located between
82 the plant sample and the pressure generator. In this paper we will refer to
83 this method as the “HPFM setup” (Tyree et al., 1993). The HPFM setup is
84 mainly used for measuring the hydraulic conductivity of roots (Tyree et al.,
85 1995; Tsuda and Tyree, 2000). Yet another modification to the Sperry method
86 was proposed by Kolb et al. (1996), who measured the hydraulic conductance
87 of entire branches or root systems by placing them in a vacuum chamber and
88 connecting the protruding stem with a water reservoir placed on a balance. In
89 this setup, water is transported through the system by suction and hydraulic
90 conductance is calculated from the linear relation between flow rate and vacuum
91 pressure in the chamber. We will refer to this method as the “Kolb setup”.

92 A method that in theory enables conductivity measurements at negative liq-
93 uid pressure is the Cavitron method (Alder et al., 1997; Cochard et al., 2013),
94 where a plant sample with rotor cups on each end is placed in a centrifuge, and
95 the pressure inside the twig is determined by the rotation rate of the centrifuge,
96 whereas the pressure gradient depends on the position of water menisci in the
97 rotor cups. The water level of the downstream rotor cup is fixed at the position
98 of its outflow hole, while the water level in the upstream rotor cup is located fur-
99 ther off-center, thus creating a gradient in water potential between the two ends
100 of the plant sample. During the experiment, the water level of the upstream

101 rotor cup slowly recedes as water is transported through the plant sample to-
 102 wards the downstream rotor cup. The flow rate could be calculated by taking
 103 the change in water level in the upstream rotor cup over time and multiplying
 104 it with the cross-sectional area of water in the rotor cup. However, due to the
 105 unknown twig volume in the rotor cup, an exact flow rate, and thus hydraulic
 106 conductivity, is not routinely determined, only the relative loss in conductivity
 107 is recorded as rotation speed is increased.

108 Unfortunately, none of the above methods reproduces the situation *in planta*:

- 109 • In the centrifuge method, the pressure along the twig is non-linear, with
 110 the lowest pressure in the middle (Cochard, 2002), rather than at the sink,
 111 as would be the case in a real plant.
- 112 • In all of the above methods, the pressure difference along the sample
 113 is held constant (atmospheric at the outflow side of the twig and above-
 114 atmospheric at the inflow side for the Sperry and HPFM setups), while the
 115 flow rate adjusts according to the hydraulic conductance of the twig. This
 116 is in contrast to natural conditions in a plant, where the system functions
 117 at sub-atmospheric or even negative liquid pressure and the pressure drop
 118 along the flow path adjusts to the hydraulic conductivity and the flow
 119 rate, the latter of which is determined by the transpiration rate (Venturas
 120 et al., 2017). This means that a sudden decline in hydraulic conductivity
 121 would cause a sudden drop in pressure, which is not the case in the above
 122 methods, which all control the pressure gradient across plant samples such
 123 that in the event of embolism propagation, the flow rate decreases, not
 124 the pressure, as would be expected in an intact plant.
- 125 • Most methods involve above-atmospheric pressures, so water stress cannot
 126 be induced while measuring hydraulic conductivity.

127 Except for the setup by Tyree and Yang (1992), none of the above methods
 128 quantifies changes in water storage of the plant sample, so it is not clear if the
 129 flow measured at one end of the sample constitutes through-flow or if part of the
 130 observed flow is due to emptying or re-filling water storage in the plant sample
 131 (Torres-Ruiz et al., 2012).

132 To fill these methodological gaps, in the present study, we aim to design
 133 an experimental setup for measuring hydraulic conductivity closer to natural
 134 conditions, with the following goals:

- 135 1. Flow rate controlled, pressure drop as response;

- 136 2. Suction-induced flow;
- 137 3. Ability to simulate water stress in the plant segment;
- 138 4. Ability to measure changes in storage.

139 3 Materials and Methods

140 Below, we present two different setups that were designed to achieve the above-
141 mentioned goals. One is an intuitive, low-cost vertical setup resembling an
142 artificial plant. The second is a more controlled horizontal setup, improving on
143 certain shortcomings of the vertical setup.

144 3.1 Artificial Plant Setup

145 The initial setup was designed to mimic a plant in the simplest form, containing
146 one evaporating “leaf”, one “root” immersed in a water reservoir, and connect-
147 ing tubes where a plant segment is inserted in a vertical setup (Fig. 1). The root
148 and leaf each is replicated by a Rhizon sampler (Rhizosphere Research Prod-
149 ucts B.V., Wageningen, Netherlands), consisting of a membrane with pores of
150 $5\mu\text{m}$ diameter. Pressure sensors (24PC; Honeywell, Morristown, NJ, USA) are
151 connected through T-valves on either side of the plant segment. A liquid flow-
152 meter (SLG-0150; Sensirion, Stäfa, Switzerland) is inserted in the flow path
153 below the lower pressure sensor. The water reservoir consists of a beaker filled
154 with de-ionized water.

155 Evaporation from the leaf replica generates the suction necessary to pull
156 water up all the way from the beaker, following the cohesion-tension principle.
157 Note that the membranes need to be covered by a continuous water film, oth-
158 erwise air can enter through empty pores and water transpired at the surface is
159 replaced by air, instead of water from below.

160 Initial filling of the system is performed without a twig in place, by placing
161 both membranes in a beaker filled with DI water. A syringe is attached to one
162 of the T-valves, at the position where the twig will be added. The syringe is
163 pulled to fill the membrane and tubing with water. Turning the T-valve to only
164 be open to the syringe and pressure sensor, the sensor is removed and water is
165 pushed to fill that section and the sensor is re-attached. The process is repeated
166 with the other side. Finally, the twig sample is attached and the setup is placed

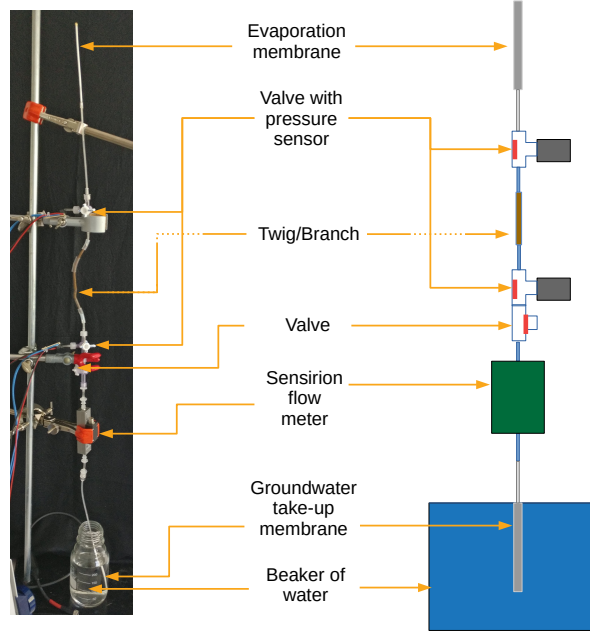


Figure 1: Setup for measuring hydraulic conductivity of twig samples using an evaporation membrane to drive flow.

upright with one membrane in the beaker and the other held in the air using a stand where it begins to evaporate (Fig. 1).

3.2 Horizontal Syringe Setup

The horizontal syringe setup (Fig. 2) consists of a syringe pump (neMESYS; Cetoni, Wiesenring, Germany) to control the flow rate through a twig sample, pressure sensors on either side of the twig, and a flow meter (SLI-0430; Sensirion, Stäfa, Switzerland). The system is water filled by pulling water from the beaker to the syringe pump through the bypass connecting the pressure sensors, then detaching the syringe to empty the air and re-attaching it.

Additionally, a capillary is connected between the water beaker and the flow meter to increase flow resistance on the upstream side and hence reduce overall pressure in the system if desired. A bypass is present, such that flow can either go through or around the capillary. This setup will be referred to as the “Syringe setup”.

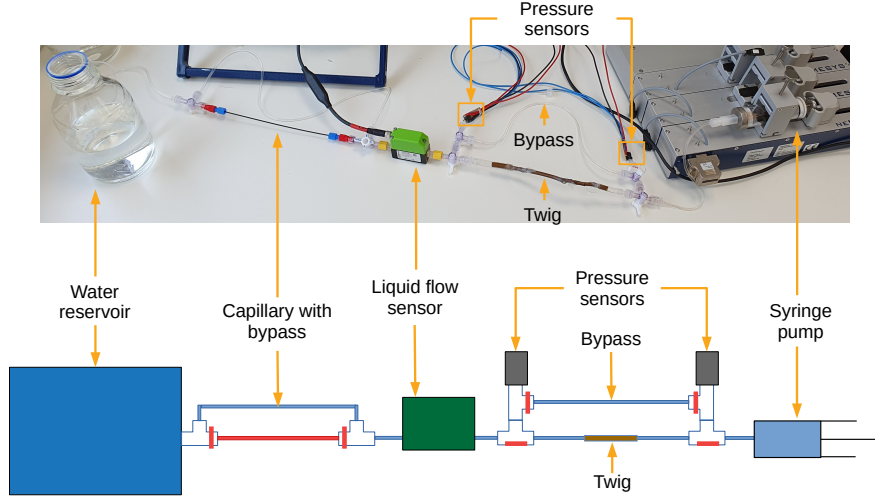


Figure 2: Horizontal syringe setup using syringe pump (g) to control water flow rate to and from the beaker (a). The twig (e) is inserted in the flow path to measure its hydraulic conductivity using flow (c) and pressure (d) meters. The bypass (f) is used to calibrate the sensors before an experiment. A capillary with bypass (b) is used as an example modification to lower the pressure.

3.3 Calibration Procedure

In this section, we describe the calibration procedures for the pressure and flow sensors. The flow sensor is calibrated before each experiment as there can be instrument drift between experiments due to biological residue build-up, which can only be eliminated by periodic flushing with alcohol. For the calibration, water flow is redirected through the bypass around the sample (Fig. 2f) with a direct path between the syringe and water reservoir. Known flow rates are generated using the syringe pump and correlated with measurements by the flow meter. The calibration is performed using a linear regression and applied to the data of the following experiment.

Pressure sensors were calibrated individually using the relation between pressure and volume obtained from the ideal gas law (Eq. 1).

$$PV = nRT \quad (1)$$

193 In Eq. 1 P is the pressure (Pa), V is the volume of the gas (m^3), n is the
 194 number of moles (mol), R is the gas constant ($\text{K mol Pa}^{-1} \text{ m}^{-3}$), and T is the
 195 temperature (K).

196 Assuming a completely sealed system (n is constant), and a constant tem-
 197 perature during the calibration, a change in the gas volume from V_{ref} to V_{new}
 198 would cause an inversely proportional change in pressure from P_{ref} to P_{new} ,
 199 such that:

$$P_{new} = \frac{P_{ref} V_{ref}}{V_{new}} \quad (2)$$

200 The pressure sensors were attached to the syringe with a small tube and
 201 t-valve which was closed to the atmosphere, the internal volume of which was
 202 considered as the reference gas volume (V_{ref}) and thus needed to be measured.
 203 To do so, we weighed the empty tube and t-valve, before and after filling it with
 204 water. By taking the weight difference between them and dividing it by the
 205 density of water, we obtained the reference gas volume.

206 The pressure sensor measures pressure relative to the atmosphere using two
 207 openings, one open to the atmosphere and one attached to the volume of in-
 208 terest. A membrane between the two openings bends with the difference in
 209 pressures and delivers a voltage based on the amount of inflection. With no
 210 difference (both at atmospheric pressure), no voltage is delivered and 0 V was
 211 measured. After filling the system with air at atmospheric pressure (assumed to
 212 be 101.3 kPa) and recording the measured sensor voltage (0 V), a known change
 213 in volume was applied using the syringe and the corresponding pressure was de-
 214 termined from Eq. 2. This pressure, along with the measured sensor voltage
 215 was recorded. This was repeated in several steps while increasing volume and
 216 decreasing volume again, in order to prevent that any transient in conditions
 217 (e.g. temperature or instrumental drift, or air leaks) would influence the slope
 218 of the calibration. Both sensors were calibrated one after another on the same
 219 day, taking 15 minutes for each sensor. In order to determine if the values of the
 220 sensors drifted over time, a second calibration was done two years later. The
 221 data of both calibration sets was pooled together, resulting in a data series of
 222 22 points for the bottom sensor, with pressures ranging between 2.56 kPa and
 223 101.3 kPa, and 21 points for the top sensor, with pressures ranging between 2.68
 224 kPa and 101.3 kPa. Linear least square fits through the data gave Pearson's
 225 correlation coefficients of $r > 0.998$ for each sensor. Due to the high correla-
 226 tion coefficients for the pooled data, suggesting minimal instrument drift, the

227 slope and intercept of the pooled calibration data were applied to all experimen-
 228 tal data presented here. Furthermore, any biases that would remain from this
 229 method cancel out when calculating the pressure difference between the sensors
 230 (ΔP) for measuring conductivity. To further counteract potential instrumental
 231 drift, before each experiment, the difference in pressure between the two sensors
 232 is measured at two points to remove any offsets. The first point is measured
 233 before an experiment when the sensors are at atmospheric pressure. The second
 234 point is the lowest attainable liquid pressure reachable with the setup, i.e. the
 235 water vapor pressure, which is measured once the experiment has concluded.
 236 The latter is measured by closing valves such that the syringe is only connected
 237 to both sensors via the bypass and flow cannot occur. The syringe is set to
 238 pull at $250 \mu\text{L min}^{-1}$, and as in-flow is stopped, pressure lowers to the vapor
 239 pressure where gas bubbles form and the pressure no longer decreases. The
 240 flow is continued for 20 minutes. The water vapor pressure measurement occurs
 241 after the experiment as the measuring process fills the setup with gas. From the
 242 two points, a linear regression of the difference between the pressure sensors is
 243 calculated and a correction is applied to remove potential offsets.

244 **3.4 Sample Collection and Connection**

245 All twig samples used in this paper were collected from *Fagus sylvatica* in Bel-
 246 val, Luxembourg, following Wheeler et al. (2013) to avoid having any artificial
 247 embolism propagation in the sample. The branch is cut from the tree and left
 248 to sit in a bag for at least 30 minutes. The branch is then re-cut under water,
 249 cutting at least one mean vessel length from either side of the sample to make
 250 sure that any embolism due to the initial cut is removed. For samples in this
 251 paper, 10 cm are removed from each end, as Buchmüller (1986) found that 40%
 252 of the dry wood samples of *Fagus sylvatica* had a maximum vessel length of un-
 253 der 8 cm, with an additional 30% of samples having a maximum vessel length
 254 between 8 and 16 cm. Any branches along the cut segment are removed under
 255 water and sealed with parafilm and/or silicon gel to avoid air entry. Flexible
 256 tubing is attached to both ends of the submerged twig, then removed from the
 257 water and connected to either side of the setup. The diameter of the samples
 258 varied between 3.8 and 4.2 mm. We did not measure the diameter for all the
 259 samples, thus a value of 4.0 mm was used for the calculations (see below).

3.5 Conductivity Calculation

Flow through a porous medium such as the twig xylem can be described using Darcy's Law (Eq. 3):

$$Q_m = \frac{kA\rho}{\mu L} \Delta P \quad (3)$$

where Q_m is the mass flow rate (kg s^{-1}), k is the intrinsic permeability (m^2), A is the cross sectional area of the whole twig (m^2), ΔP is the pressure drop along the flow path (MPa), μ is the dynamic viscosity ($\text{MPa} \cdot \text{s}$), and L is the length of the segment (m). The mass flow rate can be converted to a volumetric flow rate (Q_v , $\text{m}^3 \text{s}^{-1}$) by multiplying the mass flow rate by the density of water:

$$Q_v = \frac{Q_m}{\rho} \quad (4)$$

In the literature, the efficiency of water transport through a twig sample is expressed in different ways, which have different relations to intrinsic permeability (k) and are expressed in different units. For example, some authors use specific conductivity, which is affected by viscosity, $K_S = \frac{k\rho}{\mu}$ ($\text{kg m}^{-1} \text{MPa}^{-1} \text{s}^{-1}$), others use specific conductance, which is affected by viscosity and sample length, $K_{AS} = \frac{k\rho}{\mu L}$ ($\text{kg m}^{-2} \text{MPa}^{-1} \text{s}^{-1}$) (Caquet et al., 2009). In some cases, e.g. Bär et al. (2018); Rosner et al. (2019), the units of specific conductivity were reported as ' $\text{m}^2 \text{MPa}^{-1} \text{s}^{-1}$ ', which are obtained by substituting the volumetric flow rate (Eq. 4) for the mass flow rate in Eq. 3.

Note that viscosity is temperature dependent and therefore specific hydraulic conductivity values should only be compared between measurements performed at similar temperatures. All the experiments presented in this paper were conducted in an air conditioned lab around 21 °C and humidity between 25 and 40%. Continuous temperature measurements in a 500 ml beaker of water in the same lab revealed that the water temperature varied between 21 and 23 °C over the duration of 2 weeks in September 2022, with a maximum temporal variation by 0.6 K in 2 hours. Whenever temperature was needed for calculations, we used a temperature of 21 °C.

For easier comparison with literature values, we do not report intrinsic permeability, but calculated the specific hydraulic conductivity of twig samples

288 using the formulation of Sperry et al. (1988):

$$K = \frac{Q_V \rho L}{\Delta P A} \quad (5)$$

289 where K is the hydraulic conductivity ($\text{kg m}^{-1} \text{MPa}^{-1} \text{s}^{-1}$), ρ is the density of
 290 water (kg m^{-3}). The pressure drop (ΔP) was measured by pressure sensors on
 291 both sides of the twig, as described above. The length of the twig is measured
 292 as the distance between the centers of the cuts on each side. The cross-sectional
 293 area (A) is calculated from the stem diameter assuming a circular shape. The
 294 flow rate in the syringe setup is measured by the syringe pump (as a set flow
 295 rate out of the twig), and the flow sensor (as an instantaneous flow rate into
 296 the twig). Unless otherwise noted, the flow meter measurements were used to
 297 calculate conductivity in this paper as these resulted in more stable conductivity
 298 values (see also SI Fig. S3).

299 3.6 Experiments

300 In the first experiment, the artificial plant setup was left to evaporate to test the
 301 measurement of flow, pressure difference, and conductivity change over time.
 302 Then, we attempted to produce runaway embolism propagation by adding a
 303 gas bubble to initiate embolism. The gas bubble was the width of the tubing
 304 and 1.5 times the width in length, and was added through a valve below the
 305 lower pressure sensor and rose to the twig while flow, pressure, and hydraulic
 306 conductivity were being measured.

307 The remaining experiments were conducted using the horizontal syringe
 308 pump setup. First, the setup was compared with the current standard, the
 309 Sperry method, to verify if similar values of hydraulic conductivity are obtained
 310 using either method. For direct comparison, both methods were applied consec-
 311 utively using the same sample. The Sperry method was applied by disconnecting
 312 the syringe pump (g in Fig. 2), and letting the water drain freely while elevat-
 313 ing the beaker at the other end of the setup (a in Fig. 2) to create the desired
 314 pressure difference. The beaker was elevated to 35.5 cm for 30 minutes, then to
 315 73.5 cm for 30 minutes, then to 104.9 cm for 30 minutes, and then returned to
 316 73.5 cm for another 30 minutes, before returning to 35.5 cm for 30 minutes.

317 After this set of measurements, the beaker was placed back on the table, and
 318 the syringe pump was re-attached. Water was pulled through the sample (in the
 319 same flow direction as before) at flow a rate of $10 \mu\text{L min}^{-1}$ for 30 minutes, then

at $20 \mu\text{L min}^{-1}$ for 30 minutes, then at $30 \mu\text{L min}^{-1}$ for 30 minutes, then again at $20 \mu\text{L min}^{-1}$ for 30 minutes, before returning to $10 \mu\text{L min}^{-1}$ for another 30 minutes.

The next experiment was designed to simulate water stress in plants using the syringe setup. Two types of water stress were simulated, (a) reduced water supply (e.g. due to soil moisture drought), and (b) increased leaf water demand (e.g. in the mornings, or due to wind gusts or sunflecks). To simulate soil moisture drought, water flow between the beaker and the twig was deviated through a capillary by turning the valves in Part b of Fig. 2, resulting in increased flow resistance upstream of the twig and hence reduced pressure. Increased water demand was simulated by increasing the flow rate induced by the syringe pump, increasing the pressure gradient along the twig.

The final experiment was designed to quantify the change in twig water storage between a relaxed condition (zero flow, e.g. at night) and flow under tension (e.g. during the day). In this experiment, the syringe setup was started in the same way as in the soil moisture drought experiment, i.e. water was passed through a capillary before reaching the twig. When the measured flow rate into the twig became roughly steady, the syringe pump was stopped and the subsequent slow decay in flow rate was monitored until flow was no longer detected. Differences between syringe pump flow and the flow meter signal were interpreted as rate of change in twig storage.

4 Results

4.1 Conductivity Measurement with Artificial Plant Setup

Time in the graphs begins at 0 with the start of the experiment, which represents the first time flow was induced. This was either when the membrane was removed from water, the beaker was moved to a higher elevation, or the flow was started with the syringe pump.

A 2.2 cm long twig was attached to the artificial plant setup and left to evaporate. The flow rate started at $2.5 \mu\text{L min}^{-1}$ and increased steadily to $4.0 \mu\text{L min}^{-1}$ over the first 3.7 hours of the experiment. During this time, the pressure above the twig slowly decreased from 93 kPa to 91.5 kPa (Fig. 3). The conductivity of the sample increased from $0.023 \text{ kg m}^{-1} \text{ MPa}^{-1} \text{ s}^{-1}$ over the first hour. The air bubble was added at 1.5 hours (Fig. 3a) while conductivity continued to increase to a peak of $0.033 \text{ kg m}^{-1} \text{ MPa}^{-1} \text{ s}^{-1}$ at

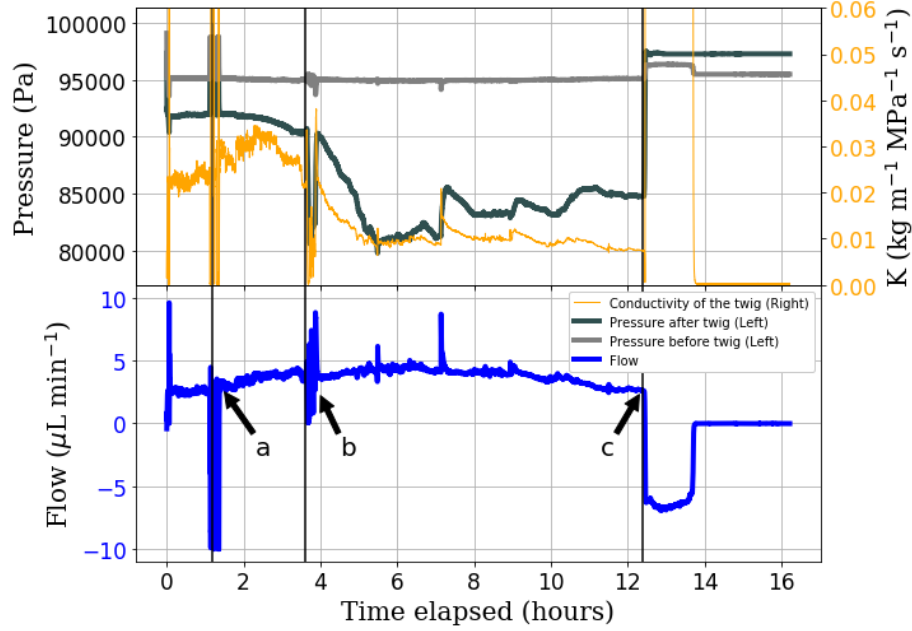


Figure 3: Flow, pressure, and conductivity measurements of a 2.2 cm *Fagus sylvatica* sample in the artificial plant setup. Air bubble was added below the lower pressure sensor 'a', and reached the sample at time 'b'. Air entered the membrane at the top and flow reversed at 'c'.

the 2.3 hour point and then decreased again to $0.027 \text{ kg m}^{-1} \text{ MPa}^{-1} \text{ s}^{-1}$ at 3.7 hours, when the bubble reached the sample. At this point, flow dropped to 0 and pressure decreased rapidly to 80.7 kPa (Fig. 3b), at which point the air bubble began passing through the twig. After 15 minutes we were able to observe air bubbles coming out of the twig on the upper side, indicating that at least part of the gas in the introduced bubble passed through the whole twig and left it again at the other end. The pressure returned to the previous 91.5 kPa, and flow resumed at $4 \mu\text{L min}^{-1}$. The flow remained relatively stable for the next 1.5 hours while both pressure and conductivity decreased markedly (from 91.5 kPa to 80.7 kPa and from 0.021 to $1.0 \times 10^{-8} \text{ kg m}^{-1} \text{ MPa}^{-1} \text{ s}^{-1}$, respectively) during this time. Both pressure and conductivity stayed relatively steady for the next 6 hours until air entered the upper membrane from outside at 12.5 hours (Fig. 3c). The upper pressure increased and flow reversed, draining water from the setup above the twig, until the water meniscus stopped at the top of the twig.

4.2 Horizontal Syringe Setup vs. Sperry Method

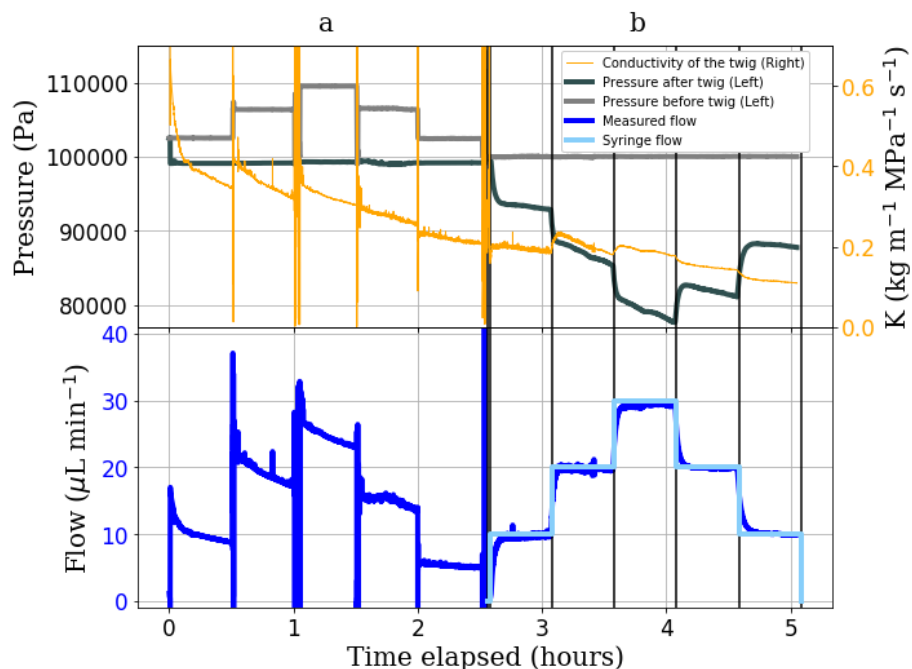


Figure 4: Pressure, flow, and conductivity measurements of a 10.2 cm twig sample over time. Section 'a' represents measurements when water is pushed through a twig sample using controlled pressure differences (Sperry method). Section 'b' represent measurements when water is pulled through the same sample in the same direction using a syringe pump (Syringe setup).

During the Sperry method (Fig. 4a), conductivity decreased steadily by 66% over the total 2.5 hours. When the pressure gradient was increased at 0.5 hours, there was a step increase in conductivity from 0.36 to 0.41 $\text{kg m}^{-1} \text{MPa}^{-1} \text{s}^{-1}$. Similar increases in conductivity were observed every time the pressure gradient was increased, but only one of two step decreases in pressure gradient resulted in an evident decline in conductivity (at 2 hrs, not at 1.5 hrs). Also when the method switched from Sperry method to Syringe at 2.5 hours, the hydraulic conductivity was not affected and remained at 0.21 $\text{kg m}^{-1} \text{MPa}^{-1} \text{s}^{-1}$ during the transition. Over the 2.5 hours of the syringe pull (Fig. 4b), conductivity also decreased (decreased 50% over 2.5 hours), but more slowly than during the Sperry method. Whenever flow rate was increased, there was a step-wise increase in conductivity, and whenever flow rate was decreased, there was a

382 slight step-wise decrease in conductivity.

383 When the different hydraulic heads where applied in the Sperry method (Fig.
384 4a), the pressure was constant and the flow rate decreased over time. However,
385 when different flow rates were applied in the Syringe method (Fig. 4b), it was
386 the pressure that decreased over time while flow was constant.

387 4.3 Simulating Water Stress

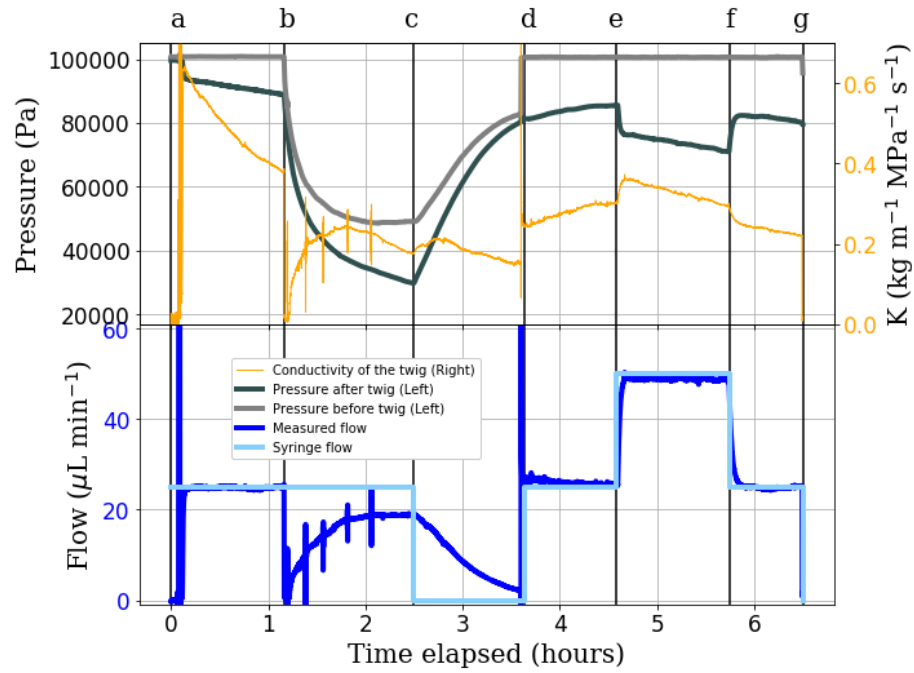


Figure 5: Time series of pressure, flow, and conductivity of a 13.5 cm twig when simulating different sorts of water stress. At ‘a’, a constant pull through the twig at $25 \mu\text{L min}^{-1}$ is applied and flow goes around the capillary. At ‘b’, flow is lead through a capillary upstream of the twig. At ‘c’, the syringe pump is stopped. At ‘d’, conditions are similar to ‘a’. At ‘e’, flow is further increased to $50 \mu\text{L min}^{-1}$. At ‘f’, the system returned to the same conditions as ‘a’ and ‘d’. The experiment ends at ‘g’.

388 In Fig. 5, the letters ‘a’ through ‘g’ indicate a change to the experimental
389 setting. In Segment ‘a-b’, a constant pull was applied through the twig at 25
390 $\mu\text{L min}^{-1}$ with no flow through the capillary, representing a steady evaporation
391 of the leaf during the day at unrestricted water supply. This reference scenario

was established in Segments ‘a-b’, ‘d-e’, and ‘f-g’, for direct comparison to the stress conditions.

Drought stress is simulated at ‘b’, where flow was redirected through a capillary upstream of the twig. In Segment ‘b-c’, flow initially stopped and pressure before the twig decreased sharply, followed by a decrease in pressure after the twig, and slow recovery of flow and conductivity, which reached $0.23 \text{ kg m}^{-1} \text{ MPa}^{-1} \text{ s}^{-1}$ before declining again. When the syringe pump was stopped at ‘c’, flow decreased from 19 to $3 \text{ }\mu\text{L min}^{-1}$ over the course of an hour, in Segment ‘c-d’, while pressures increased. Conductivity remained similar to that in Segment ‘a-b’, around $0.20 \text{ kg m}^{-1} \text{ MPa}^{-1} \text{ s}^{-1}$.

At ‘d’, the syringe pump was turned on again and the capillary bypassed, as in Segment ‘a-b’. When the pump was turned on, flow rate increased instantly, accompanied by a step increase in conductivity from 0.15 to $0.26 \text{ kg m}^{-1} \text{ MPa}^{-1} \text{ s}^{-1}$. Note that the measured flow rate was initially even higher than the syringe pump flow rate in Segment ‘d’.

Increase in water demand was simulated at ‘e’, where water flow through the twig was increased from 25 to $50 \text{ }\mu\text{L min}^{-1}$. The flow change was immediately reflected by the flow meter and pressure after the twig decreased suddenly from 85 kPa to 74 kPa , while the conductivity increased from 0.30 to $0.35 \text{ kg m}^{-1} \text{ MPa}^{-1} \text{ s}^{-1}$, followed by a steady decline in Segment ‘e-f’ from 0.35 to $0.30 \text{ kg m}^{-1} \text{ MPa}^{-1} \text{ s}^{-1}$.

Once the original flow of $25 \text{ }\mu\text{L min}^{-1}$ was re-established at ‘f’, pressure after the twig increased again to almost its original value at ‘e’, whereas conductivity showed another step decrease from 0.29 to $0.26 \text{ kg m}^{-1} \text{ MPa}^{-1} \text{ s}^{-1}$. Conductivity in Segment ‘f-g’ decreased steadily from 0.26 to $0.22 \text{ kg m}^{-1} \text{ MPa}^{-1} \text{ s}^{-1}$. The overall decrease in conductivity throughout the experiment could be seen in Fig. 4-6.

4.4 Twig water storage

To better understand if the deviations between syringe pump and flow meter flow rates observed in the previous experiment were related to changes in twig water storage, Segments ‘a-d’ were repeated with a new twig, but with a longer period without syringe pump flow at the end. Changes in storage were calculated as the cumulative difference between the flow rates at the syringe pump and the flow meter.

At the start of the storage experiment (Fig. 6 Segment ‘a-b’), the same

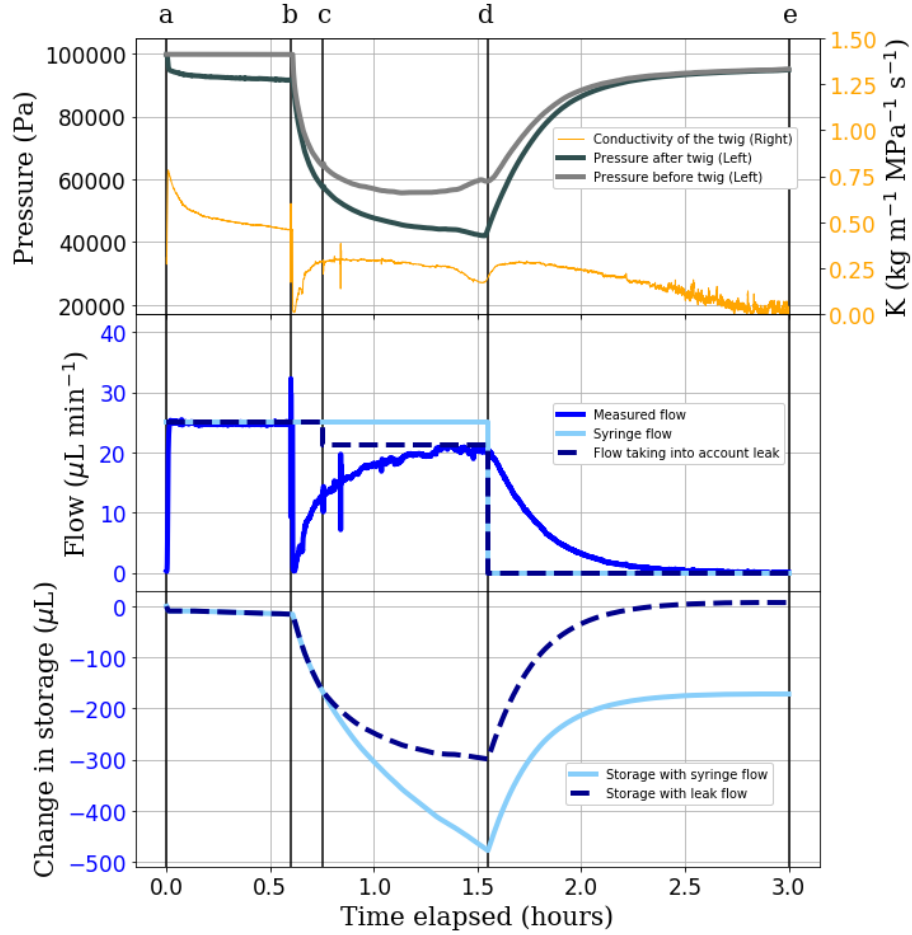


Figure 6: Graph of pressure, flow, conductivity, and storage changes when simulating water stress on a 11.4 cm twig. At ‘a’, a constant pull through the twig at $25 \mu\text{L min}^{-1}$ was applied and flow went around the capillary. At ‘b’, flow was lead through the capillary. At ‘d’, flow was stopped. The experiment ended at ‘e’. Change in storage was calculated as the cumulative difference between measured flow and syringe flow. An air leak was assumed to have formed at ‘c’, see main text.

427 pattern of declining conductivity as in the stress experiment was found. When
 428 the flow was passed through the capillary at ‘b’, the measured flow rate briefly
 429 declined to 0, followed by a steady recovery, reaching a steady rate of 21.7
 430 $\mu\text{L min}^{-1}$ at ‘d’, $3.3 \mu\text{L min}^{-1}$ lower than the syringe flow. Interpreting the
 431 difference in flow rates as a change in twig water storage, this would suggest

that the amount of water in the twig decreased by $475\ \mu\text{L}$ at ‘d’. When the syringe pump was turned off (Segment ‘d-e’) the flow meter kept recording flow into the twig, suggesting re-filling of the twig water storage until the flow ceased entirely after another 1.5 hours. At this point, our calculation would suggest a remaining twig water deficit of $175\ \mu\text{L}$ (light blue line in bottom panel of Fig. 6).

The difference between the steady state flow rate measured by the flow meter at ‘d’, and the flow rate imposed by the syringe pump suggests that a leak occurred in the system, as a steady-state difference cannot be explained by changing storage. In addition, we observed a bubble in the syringe, confirming the presence of an air leak. The leak was assumed to have formed at ‘c’ due to a slight kink in the pressure, which would likely occur when air entry is initiated. In the absence of more detailed information, the air entry rate was assumed constant in Segment ‘c-d’ and to be equal to the flow rate difference between the steady state flow at ‘d’ and the syringe flow. Using the flow rate based on the assumed air entry rate, storage would have decreased by a maximum of $300\ \mu\text{L}$ at ‘d’ and the end storage at ‘e’ would have been $7\ \mu\text{L}$ larger than the initial twig water storage at ‘a’.

5 Discussion

In this paper we presented two different methods for measuring hydraulic conductivity under suction and flow-controlled conditions. The first method is an intuitive representation of an artificial plant as an evaporating leaf, transport tissues, and a root, but it does not offer precise control of the flow. In numerous experiments using this method (not all shown here), we found that stable flow could be maintained for many hours, but invariably, sudden, catastrophic failure occurred by air entry through the evaporating microporous membrane after many hours. An interesting feature of this setup is its educational value, as its vertical orientation and components are intuitively associated with key macroscopic components of the plant hydraulic system. In this evaporation-driven experimental setup, flow rate continued even when the flow was temporarily constricted, providing the inspiration for a fully flow controlled horizontal setup using a syringe pump to control the flow (second method).

This second method is of more scientific value, as it allows for more precise control of flow rate and quantification of twig storage changes as flow rates are

466 known for both sides of the twig. Estimations of twig water storage changes
 467 can also be enabled by adding a second balance in the Sperry setup (Tyree
 468 and Yang, 1992), but here we avoid evaporation from the beakers, which could
 469 cause artifacts in the flow measurements. Our method combines the advantage
 470 of quantifying changes in twig water storage with the advantage of measuring
 471 conductivity by suction instead of above-atmospheric pressure, as proposed by
 472 Kolb et al. (1996), who pointed out that the large pressures needed to measure
 473 samples with low conductance (e.g. due to partial embolism) would lead to re-
 474 filling of embolised vessels and therefore over-estimate conductance. Therefore,
 475 measurements under suction are expected to lead to more accurate hydraulic
 476 conductivity values. Since the pressure is measured on both sides of the twig
 477 in our setup, we can add an additional resistance (such as a capillary) to the
 478 upstream side of the twig to reduce the pressure in the twig. Note that although
 479 a sub-atmospheric pressure could also be achieved by elevating the twig relative
 480 to the water reservoirs in the setup by Tyree and Yang (1992), for the pressure
 481 drop of 70 KPa shown in Fig. 5, the twig would have to be elevated to a height
 482 of 7 m, so that setup can only be used for very mild reductions in pressure. In
 483 essence, our second method combines the advantages of both setups presented
 484 by Tyree and Yang (1992) and Kolb et al. (1996), with the additional bonus
 485 of controlling flow while the pressures adjust, which is more representative of a
 486 situation where flow is driven by evaporation.

487 The two setups presented here are able to provide different scientific in-
 488 sights and highlight different challenges for the quantitative understanding of
 489 flow through plant segments. In the artificial plant setup, where we introduced
 490 an air bubble below the twig, we were able to see a sudden decline in liquid
 491 pressure on the leaf side as the bubble reached the twig, but then, surprisingly,
 492 as the pressure difference reached a threshold of 15 kPa (Fig. 3b), the bubble
 493 started entering the twig and pressure returned to its original value within tens
 494 of minutes. Contrary to expectations that air entry would lead to reduced or
 495 discontinued flow through the hydraulic system, flow and evaporation continued
 496 at the original rate throughout this experiment, with only short-term pertur-
 497 bations when the bubble was introduced and when it passed through the twig.
 498 This was despite a marked decrease in hydraulic conductivity from 0.035 to
 499 $0.010 \text{ kg m}^{-1} \text{ MPa}^{-1} \text{ s}^{-1}$ during the experiment. It is not clear if the decline in
 500 hydraulic conductivity was caused by the added air or independent of it, as the
 501 decreasing trend was observed before the bubble reached the twig, and the same
 502 trend continued after it had passed through the twig. Note that the behavior

documented here was only observed with a twig that was shorter than its average xylem vessel length (here a twig of 2.2 cm was used, cf. an average xylem vessel length of under 8 cm for *Fagus sylvatica* (Buchmüller, 1986)). When a longer twig of 12.3 cm was used (SI, Fig. S2), flow declined to zero shortly after the bubble reached the lower twig end after 4.2 hours. In this case, the bubble did not pass through the twig, blocking flow completely and eventually leading to air entry through the evaporating membrane and failure after 5.9 hours (SI, Fig. S2). This illustrates that there was no vessel longer than 12.3 cm present in the sample, and that air could not pass from one vessel to another, such that flow was completely blocked. In the artificial plant setup, any gas bubbles transported with the water accumulated at the top of the artificial leaf, presumably allowing water supply to the evaporating sites only through a thin film along the membrane. This increased resistance to flow likely created a large pressure drop between the bulk water and the evaporating sites at the tip, eventually resulting in air entry at the top of the membrane. When the air entry value of the evaporating membranes was tested without a twig and air bubbles, we found sudden air entry at liquid pressures between 35 and 57 kPa, which is consistent with the reported pore sizes of the membrane (see SI, Fig. S1). The accumulation of air bubbles at the evaporating sites and subsequent hydraulic failure highlights the importance of mechanisms to not let air bubbles accumulate in the hydraulic system, even in the absence of negative liquid pressures.

To avoid hydraulic failure of the system due to accumulation of air in the evaporation membrane and fluctuations in flow rate due to variations in lab humidity or air movement around the evaporating membrane, we developed the horizontal syringe setup, which also improves on the previous design by arranging the setup horizontally, and hence avoiding the offset between pressure sensors due to gravitational potential and ensuring that the pressure difference measured by the sensors does actually represent the pressure drop along the twig. Note that branches can grow horizontally, so a horizontal setup is not less “natural” than a vertical one. The replacement of the evaporation membrane by a syringe pump eliminates the pressure limitation due to the membrane’s air entry pressure, and fluctuations in flow caused by fluctuations in evaporation from the membrane. For the same reason, the use of a rhizon on the water uptake side was also abandoned. The original idea was to place the rhizon in a porous material to simulate the reduced liquid pressure exerted by the soil, but with the rhizons used, the pressure could not be lowered below the air entry

540 pressure of the membrane. Instead, a capillary was used to reduce pressure on
 541 receiving side of the twig. The syringe pump allows the flow rate to be precisely
 542 controlled through either suction or pushing, as opposed to the evaporation
 543 from the membrane. The horizontal syringe setup and the Sperry method gave
 544 comparable values for hydraulic conductivity of the same sample (Fig. 4). Fur-
 545 thermore, the overall trend in the conductivity over time is maintained when
 546 swapping between the two methods. The step increase and decrease patterns,
 547 when changing pressure difference or flow rate, were seen in both methods, sug-
 548 gesting that the results are likely not of methodological nature, but biological.
 549 The specific hydraulic conductivity was measured between 0.20 and 0.60 kg
 550 $\text{m}^{-1} \text{MPa}^{-1} \text{s}^{-1}$, 3 to 4.5 times lower than literature values: 2.5 kg $\text{m}^{-1} \text{MPa}^{-1}$
 551 s^{-1} in Rosner et al. (2019) using the Sperry method, and 1.83 kg $\text{m}^{-1} \text{MPa}^{-1}$
 552 s^{-1} in the Xylem functional traits database (<https://xylemfunctionaltraits.org/>)
 553 Choat et al. (2012). As pointed out by Kolb et al. (1996), the higher conductiv-
 554 ity values reported in the literature could be due to the filling of empty vessels
 555 when samples were flushed with water at high pressures.

556 In all our experiments, we observed continuous declines in hydraulic conduc-
 557 tivity during measurements, which have also been reported before and largely
 558 attributed to microbial growth (Sperry et al., 1988). To avoid the decline in
 559 hydraulic conductivity and to mimic xylem sap, it has been suggested to add
 560 HCl, KCl, and oxalic acid to the perfusing solution (Sperry et al., 1988; Kolb
 561 et al., 1996; Nardini et al., 2011). Here we note that the previously reported
 562 declines were over timescales of tens of hours (Sperry et al., 1988), whereas our
 563 experiments only lasted a few hours. Therefore we used distilled water and were
 564 surprised to see the largest declines within the first half-hour in our horizontal
 565 experiments (Figs. 4 - 6). Note that in our vertical experiments, where the flow
 566 rate was much lower, the initial decline in conductivity was not observed (Fig.
 567 3 and Fig. S1). This could imply that the decline in hydraulic conductivity
 568 was not so much due to microbial growth as to the accumulation of bubbles at
 569 the pit membranes (Canny et al., 2007). More experiments using different flow
 570 rates would be needed to separate these processes more clearly.

571 The comparable hydraulic conductivity measurements between the Sperry
 572 method and the horizontal syringe setup, along with approximately similar re-
 573 sults to literature values confirm that the horizontal Syringe method is a valid
 574 alternative to the Sperry method for measuring hydraulic conductivity. In addi-
 575 tion, the syringe setup was able to measure hydraulic conductivity while simu-
 576 lating water stress conditions. Simulated soil moisture stress caused a decrease

577 in the pressure on both sides of the twig sample (Fig. 5), which is not possible
 578 using the Sperry or HPFM methods, as they rely on fixed pressure gradients
 579 and above-atmospheric pressure. Surprisingly, our experiment showed that an
 580 increase in flow rate increased the conductivity of the sample, both at constant
 581 pressure difference (Sperry method) and constant flow rate (Syringe method).
 582 Conversely, step decreases in flow rate resulted in step reductions in conductiv-
 583 ity in three out of four cases in Fig. 4. Since flow rates are positively correlated
 584 with pressure in the Sperry method (increase in pressure drives flow), but nega-
 585 tively correlated with pressure in the Syringe method (increase in suction drives
 586 flow), the combination of both methods enables the conclusion that the sam-
 587 ple’s conductivity indeed depends on the flow rate, not the liquid pressure. The
 588 positive correlation between flow rate and hydraulic conductivity was also found
 589 in Fig. 5, at the transitions marked as d, e, and f. More targeted experiments
 590 on different species could shed light into potential mechanistic reasons for this
 591 behaviour.

592 Another advantage of the syringe pump setup is that the flow rate is mea-
 593 sured on both sides of the twig, giving additional information about the state
 594 of experiments. When pulling water through a sample, the water leaving the
 595 twig is determined by the syringe pump, while the flow entering the twig is
 596 measured by the liquid flow meter at the other end. In our experiments, it has
 597 enabled the detection of leaks or changes in the twig’s storage (Fig. 6). The
 598 following processes can cause a deviation between the measured flow (Q_m) and
 599 the syringe pump flow rate (Q_s):

- 600 1. Changes in water storage of the system between the flow meter and the
 601 syringe pump. This could result in $Q_m > Q_s$ or $Q_m < Q_s$.
- 602 2. Evaporation of water from the twig. This would result in $Q_m > Q_s$.
- 603 3. Air seeding or exsolution of gas between the flow meter and the syringe
 604 pump. This would result in $Q_m < Q_s$. Air bubbles should become visible
 605 in the tubes or the syringe pump in this case.

606 To quantify the storage changes in the tubing, we ran an experiment similar
 607 to Fig. 6, but without a twig. The results suggested that a significant deviation
 608 in flow rates between the syringe pump and flow meter could only be maintained
 609 for a few minutes and the total change in storage was less than 60 μL (SI Fig.
 610 S4). Since we never observed persistently greater flow meter values compared
 611 to the syringe pump, we can exclude a significant contribution of evaporation

612 from the twig. The only occurrences of $Q_m > Q_s$ were found for a limited
 613 time after reductions in flow rate, implicating changes in storage as the reason.
 614 In two cases, we documented persistently $Q_m < Q_s$, both under conditions
 615 of low pressure, and associated with the accumulation of gas in the syringe,
 616 indicating that air might have entered. In general, if Q_m deviates from Q_s but
 617 then converges, this indicates that the system storage is adjusting to a new
 618 steady state. In Figs. 5 and 6, we found clear indications of changes in storage,
 619 some of which were followed by indications of temporary leaks or gas exsolution
 620 periods (persistently $Q_m < Q_s$ in Fig. 5b-c, and Fig. 6c-d). In Fig. 6, we
 621 calculated the change in storage from the cumulative sum of $Q_s - Q_m$ and used
 622 the steady value of $Q_s - Q_m$ in Fig. 6c to quantify the hypothesized air entry
 623 rate. Remarkably, when accounting for this air entry, assumed to occur only
 624 at a liquid pressure below 55 kPa (based on a slight bump in the pressure and
 625 flow data at this threshold), the storage deficit gradually returned to zero 1.5
 626 hours after switching the syringe pump off. This indicates the capacity of the
 627 twig to reversibly reduce and replenish its storage depending on the flow rate
 628 and pressure applied.

629 This elastic storage component may also be the reason for the so-called
 630 ‘passive water uptake’ commonly found when using the Sperry method, which
 631 is then subtracted from the measured flow rates to achieve more consistent
 632 results (Torres-Ruiz et al., 2012). Since the magnitude of the ‘passive water
 633 uptake’ increases with the xylem tension prior to the experiment (Table 1 in
 634 Torres-Ruiz et al., 2012), it is likely that the underlying mechanism is the same
 635 as that causing water flow into the twig in our experiments at zero syringe
 636 pump flow rate after the water stress treatments (Figs. 5 and 6). The dynamic
 637 decay of this spontaneous water uptake observed in our experiments is consistent
 638 with the interpretation that it is likely related to a relaxation of elastic tissues
 639 (Zweifel et al., 2001). However, since the dynamics of flow during a conductivity
 640 measurement is usually not reported, we cannot tell in how far the ‘passive
 641 water uptake’ analysed by Torres-Ruiz et al. (2012) is indeed related to the
 642 elastic relaxation seen in our experiments, and if it was, how a constant rate
 643 of ‘passive water uptake’ could be deduced from such a dynamically decaying
 644 curve. Fortunately, the ability to measure flow rate on both sides of the twig in
 645 our setup gives us a clear indication of any artifacts in the flow measurements,
 646 and to our surprise, conductivity calculations based on the measured flow rate of
 647 water into the twig and the pressure gradient along the twig produced consistent
 648 conductivity values even during moderate emptying or re-filling of the twig water

reservoir (see e.g. conductivity values before and after Point d in Fig. 6). Note that the change in storage of our system without a twig is an order of magnitude smaller than the change in storage observed in the presence of a twig (SI Fig. S4 and S5), so we can rule out an artifact due to elasticity in our system.

The experiments presented here were not designed to gain any particular scientific insights, but to illustrate the capabilities and potential limitations of the newly presented methods. The main limitation of both methods is that the liquid pressure cannot be lowered sufficiently to induce significant loss of conductivity during a flow measurement. Even if the valve upstream of the twig is closed while the syringe pump is sucking, liquid pressure only decreases down to the saturation vapour pressure of the water in the tubes, i.e. around 3 kPa at 25 °C, at which point cavitation occurs, triggered by any gas bubble in the system, including those inside the pressure sensors. Conducting flow and pressure measurements below this pressure, or even at negative pressures in the MPa range, as expected in plants, would require removal of all gas bubbles and any cavitation nuclei in the system, which has so far only been achieved in microscopic systems (Wheeler and Stroock, 2008; Pagay et al., 2014). Nevertheless, even at the modest range of sub-atmospheric pressures attainable in the current setup, we have been able to observe transient changes in twig water storage lasting for up to an hour, suggesting that this setup could be used to not only measure the hydraulic conductivity of plant segments very accurately, but also gain a better understanding of the role of water storage in the plant hydraulic system.

6 Conclusions

Current methods of measuring hydraulic conductivity of plant segments are based on controlling a pressure gradient and pushing water through samples, which does not reflect natural water transport processes in plants, i.e. suction-driven flow with a pressure gradient determined by the flow rate imposed by leaf water demand. Here we describe two new experimental approaches to measure hydraulic conductivity using suction and a controlled flow rate. The artificial plant setup, consisting of an artificial root, an artificial leaf and a plant segment in the flow path between the two, is well suited for educational purposes, as its components are intuitively comparable to real plant organs. The syringe pump setup, where the evaporating artificial leaf is replaced by a syringe pump, is more versatile for conducting scientific experiments. Our detailed tests of the setup

confirmed that the conductivity values obtained are similar to those measured with the traditional Sperry method when similar flow rates are used. However, due to the use of a flow meter before the twig and syringe pump controlled suction at the other end, the setup enables quantifying changes in twig water storage. We found that simulating water stress by increasing flow resistance at the source or flow rate at the sink both resulted in transient withdrawal of water from the twig, which was largely reversible, i.e. the twig replenished its storage to the original value when original flow conditions were restored. This enables unique insights into the interplay between pressure, flow rate, hydraulic conductivity and water storage in plant segments.

7 Data availability

All data and analysis code will be published on zenodo.org and at <https://renkulab.io> upon publication.

References

- Alder, N. N., Pockman, W. T., Sperry, J. S., and Nuismer, S. (1997). Use of centrifugal force in the study of xylem cavitation. *Journal of Experimental Botany*, 48(3):665–674.
- Bär, A., Nardini, A., and Mayr, S. (2018). Post-fire effects in xylem hydraulics of *Picea abies*, *Pinus sylvestris* and *Fagus sylvatica*. *New Phytologist*, 217(4):1484–1493. Publisher: John Wiley & Sons, Ltd.
- Buchmüller, K. S. (1986). Jahrringcharakteristik und Gefäßslängen in *Fagus sylvatica* L.I. *Vierteljahrsschrift der Naturforschenden Gesellschaft in Zürich*, 131(3):161–182.
- Canny, M. J. (1998). Transporting water in plants. *American Scientist*, 86:152–159.
- Canny, M. J., Sparks, J. P., Huang, C. X., and Roderick, M. L. (2007). Hypothesis: Air embolisms exsolving in the transpiration water—the effect of constrictions in the xylem pipes. *Functional plant biology*, 34(2):95–111.
- Caquet, B., Barigah, T. S., Cochard, H., Montpied, P., Collet, C., Dreyer, E., and Epron, D. (2009). Hydraulic properties of naturally regenerated beech saplings respond to canopy opening. *Tree Physiology*, 29(11):1395–1405. Publisher: Oxford Academic.
- Choat, B., Jansen, S., Brodribb, T. J., Cochard, H., Delzon, S., Bhaskar, R., Bucci, S. J., Feild, T. S., Gleason, S. M., Hacke, U. G., Jacobsen, A. L., Lens, F., Maherali, H., Martínez-Vilalta, J., Mayr, S., Mencuccini, M., Mitchell, P. J., Nardini, A., Pittermann, J., Pratt, R. B., Sperry, J. S., Westoby, M., Wright, I. J., and Zanne, A. E. (2012). Global convergence in the vulnerability of forests to drought. *Nature*, 491(7426):752–755. Number: 7426 Publisher: Nature Publishing Group.
- Cochard, H. (2002). A technique for measuring xylem hydraulic conductance under high negative pressures. *Plant, Cell & Environment*, 25(6):815–819. eprint: <https://onlinelibrary.wiley.com/doi/pdf/10.1046/j.1365-3040.2002.00863.x>.
- Cochard, H., Badel, E., Herbette, S., Delzon, S., Choat, B., and Jansen, S. (2013). Methods for measuring plant vulnerability to cavitation: a critical review. *Journal of Experimental Botany*, 64(15):4779–4791.

- 729 Dixon, H. H. and Joly, J. (1895). On the ascent of sap.
- 730 Hölttä, T., Cochard, H., Nikinmaa, E., and Mencuccini, M. (2009). Capacitive
731 effect of cavitation in xylem conduits: results from a dynamic model. *Plant,*
732 *Cell & Environment*, 32(1):10–21.
- 733 Kolb, K., Sperry, J., and Lamont, B. (1996). A method for measuring xylem hy-
734 draulic conductance and embolism in entire root and shoot systems. *Journal*
735 *of Experimental Botany*, 47(304):1805–1810. Publisher: Oxford University
736 Press.
- 737 McDowell, N. G., Brodribb, T. J., and Nardini, A. (2019). Hydraulics in the 21
738 st century. *New Phytologist*, 224(2):537–542.
- 739 Nardini, A., Salleo, S., and Jansen, S. (2011). More than just a vulnerable
740 pipeline: xylem physiology in the light of ion-mediated regulation of plant
741 water transport. *Journal of Experimental Botany*, 62(14):4701–4718.
- 742 Pagay, V., Santiago, M., Sessoms, D. A., Huber, E. J., Vincent, O., Pharkya,
743 A., Corso, T. N., Lakso, A. N., and Stroock, A. D. (2014). A microtensiome-
744 ter capable of measuring water potentials below -10 MPa. *Lab on a Chip*,
745 14(15):2806–2817. Publisher: The Royal Society of Chemistry.
- 746 Rosner, S., Heinze, B., Savi, T., and Dalla-Salda, G. (2019). Prediction of
747 hydraulic conductivity loss from relative water loss: new insights into water
748 storage of tree stems and branches. *Physiologia Plantarum*, 165(4):843–854.
749 Publisher: John Wiley & Sons, Ltd.
- 750 Shi, W., Dalrymple, R. M., McKenny, C. J., Morrow, D. S., Rashed, Z. T.,
751 Surinach, D. A., and Boreyko, J. B. (2020). Passive water ascent in a tall,
752 scalable synthetic tree. *Scientific Reports*, 10(1).
- 753 Sperry, J. S. (1986). Relationship of Xylem Embolism to Xylem Pressure Po-
754 tential, Stomatal Closure, and Shoot Morphology in the Palm *Rhapis excelsa*
755 1. *Plant Physiology*, 80(1):110–116.
- 756 Sperry, J. S., Donnelly, J. R., and Tyree, M. T. (1988). A method for measuring
757 hydraulic conductivity and embolism in xylem. *Plant, Cell & Environment*,
758 11(1):35–40.
- 759 Torres-Ruiz, J. M., Sperry, J. S., and Fernández, J. E. (2012). Improving
760 xylem hydraulic conductivity measurements by correcting the error caused

- by passive water uptake. *Physiologia Plantarum*, 146(2):129–135. _eprint: <https://onlinelibrary.wiley.com/doi/pdf/10.1111/j.1399-3054.2012.01619.x>.
- Tsuda, M. and Tyree, M. T. (2000). Plant hydraulic conductance measured by the high pressure flow meter in crop plants. *Journal of Experimental Botany*, 51(345):823–828.
- Tyree, M. T., Patiño, S., Bennink, J., and Alexander, J. (1995). Dynamic measurements of roots hydraulic conductance using a high-pressure flowmeter in the laboratory and field. *Journal of Experimental Botany*, 46(1):83–94.
- Tyree, M. T., Sinclair, B., Lu, P., and Granier, A. (1993). Whole shoot hydraulic resistance in *Quercus* species measured with a new high-pressure flowmeter. *Annales des Sciences Forestières*, 50(5):417–423. Publisher: EDP Sciences.
- Tyree, M. T. and Sperry, J. S. (1988). Do Woody Plants Operate Near the Point of Catastrophic Xylem Dysfunction Caused by Dynamic Water Stress?: Answers from a Model. *Plant Physiology*, 88(3):574–580.
- Tyree, M. T. and Yang, S. (1992). Hydraulic Conductivity Recovery versus Water Pressure in Xylem of *Acer saccharum*. *Plant Physiology*, 100(2):669–676. Publisher: American Society of Plant Biologists (ASPB).
- Tyree, M. T. and Zimmermann, M. H. (2002). The Cohesion-Tension Theory of Sap Ascent. In Tyree, M. T. and Zimmermann, M. H., editors, *Xylem Structure and the Ascent of Sap*, Springer Series in Wood Science, pages 49–88. Springer, Berlin, Heidelberg.
- Venturas, M. D., Sperry, J. S., and Hacke, U. G. (2017). Plant xylem hydraulics: What we understand, current research, and future challenges. *Journal of Integrative Plant Biology*, 59(6):356–389. _eprint: <https://onlinelibrary.wiley.com/doi/pdf/10.1111/jipb.12534>.
- Wheeler, J. K., Huggett, B. A., Tofte, A. N., Rockwell, F. E., and Holbrook, N. M. (2013). Cutting xylem under tension or supersaturated with gas can generate PLC and the appearance of rapid recovery from embolism. *Plant, Cell & Environment*, 36(11):1938–1949. _eprint: <https://www.onlinelibrary.wiley.com/doi/pdf/10.1111/pce.12139>.
- Wheeler, T. D. and Stroock, A. D. (2008). The transpiration of water at negative pressures in a synthetic tree. *Nature*, 455(7210):208–212.

- 793 Zimmermann, U., Haase, A., Langbein, D., and Meinzer, F. (1993). Mecha-
794 nisms of Long-Distance Water Transport in Plants: A Re-Examination of
795 Some Paradigms in the Light of New Evidence. *Philosophical Transactions:*
796 *Biological Sciences*, 341(1295):19–31.
- 797 Zweifel, R., Item, H., and Häslar, R. (2001). Link between diurnal stem radius
798 changes and tree water relations. *Tree Physiology*, 21(12-13):869–877.